Propulsion and Power Research 2013;2(2):148–161

http://ppr.buaa.edu.cn/

Propulsion and Power Research

www.sciencedirect.com

ORIGINAL ARTICLE

Turbine blade temperature calculation and life estimation - a sensitivity analysis

Majid Rezazadeh Reyhani[a,*], Mohammad Alizadeh[b], Alireza Fathi[c], Hiwa Khaledi[d]

[a]*Amirkabir University of Technology (Tehran Polytechnic), Tehran, 15875-4413, Iran*
[b]*School of Mechanical Engineering, College of Engineering, University of Tehran, Tehran, 4563-11155, Iran*
[c]*K.N.T University, Tehran, 19697-64499, Iran*
[d]*Sharif University of Technology, Tehran, 11365-11155, Iran*

Received 17 August 2012; accepted 16 January 2013
Available online 31 May 2013

KEYWORDS

Conjugate heat transfer;
Life assessment;
Sensitivity analysis;
Gas turbine;
Blade

Abstract The overall operating cost of the modern gas turbines is greatly influenced by the durability of hot section components operating at high temperatures. In turbine operating conditions, some defects may occur which can decrease hot section life. In the present paper, methods used for calculating blade temperature and life are demonstrated and validated. Using these methods, a set of sensitivity analyses on the parameters affecting temperature and life of a high pressure, high temperature turbine first stage blade is carried out. Investigated uncertainties are: (1) blade coating thickness, (2) coolant inlet pressure and temperature (as a result of secondary air system), and (3) gas turbine load variation. Results show that increasing thermal barrier coating thickness by 3 times, leads to rise in the blade life by 9 times. In addition, considering inlet cooling temperature and pressure, deviation in temperature has greater effect on blade life. One of the interesting points that can be realized from the results is that 300 hours operation at 70% load can be equal to one hour operation at base load.

*Corresponding author: Tel.: +98 21 88333502.
E-mail address: m_rezazadeh@aut.ac.ir (Majid Rezazadeh Reyhani)

Peer review under responsibility of National Laboratory for Aeronautics and Astronautics, China.

Production and hosting by Elsevier

1. Introduction

Increasing turbine inlet temperature is a means of improving efficiency, but this temperature exceeds allowable temperature of metal parts. In addition, the gas turbine hot parts operate in a harmful condition of centrifugal and gas pressure forces and thermal cycling. Subsequently, most

2212-540X © 2013 National Laboratory for Aeronautics and Astronautics. Production and hosting by Elsevier B.V. All rights reserved.
http://dx.doi.org/10.1016/j.jppr.2013.04.004

Nomenclature

b	fatigue strength exponent
C	specific heat
c	fatigue ductility exponent
D	life fraction
E	modulus of elasticity
h	heat transfer coefficient
k	thermal conductivity
Ma	Mach number
N_f	number of cycles to failure
n	number of cycles
$\dot{m}$	mass flow rate
P	pressure
T	temperature
t_r	time to rupture

Greek letters

ε	strain
ε'	fatigue ductility coefficient
σ	stress
σ'	fatigue strength coefficient
ρ	density
δ	thickness

Subscripts

c	coolant
co	coating
in	inlet
me	metal
out	outlet
ref	reference
s	static condition
t	total condition

Abbreviations

CHT	conjugate heat transfer
LMP	Larson-Miller parameter
SAS	secondary air system
TBC	thermal barrier coating

of the life problems are encountered in this area. Blade metal temperature distribution and temperature gradients are the most important parameters determining blade life. Therefore, accurately predicting blade heat transfer parameters is essential for precisely predicting blade life.

As mentioned above, one of the most important loads for calculating blade life is temperature distribution. In cooled turbines, in order to calculate blade temperature precisely, internal coolant, external hot gas, and metal conduction should be simulated simultaneously by conjugate heat transfer (CHT) method. There have been increased research efforts in applying the CHT methodology to simulate gas turbine blade heat transfer. Some of them are on modeling C3X and MarkII vanes in a single solver [1–7]. Although three-dimensional (3-D) modeling of vanes and blades with complex cooling passages is time-consuming, there are some studies [8–11] which used 3-D solver and CHT method to calculate the temperature distribution of vanes and blades with more complex internal cooling passages.

In addition, there are some studies [12–16] in which blade simulated by conjugate (or coupled) heat transfer method using one-dimensional (1-D) simulation for internal cooling passages. Short calculation time is the most important reason that in these works, 1-D solver is used for simulation of internal cooling passages. Dewey and Hulshof [12] carried out aero-thermal analysis for combustion turbine F-Class life prediction. In order to get both temperatures and stresses right, they used combination of through-flow (BLADE-CT) and computational fluid dynamics (CFD) (FLOTRAN) to analyze the external gas flow, the Cooling Passage Flow (CPF) program to perform the cooling flow analysis and ANSYS program to analyze the heat conduction to calculate distribution of temperatures and stress. Zecchi et al. [13] presented a simulation tool to analyze cooling system of gas turbine. This tool couples energy, momentum and mass flow conservation equations together with experimental correlations for heat transfer and pressure losses. They validated this tool with experimental data using conjugate heat transfer methodology. In addition, they carried out sensitivity analysis to boundary conditions variation in order to show how uncertainty on data can affect metal temperature distribution. Takahashi et al. [14] performed a 3-D steady-state numerical analysis of thermal conjugation for inside and outside fields of the blade, which consists of convection heat transfer around the blade, thermal conduction in the blade material combined with a one-dimensional thermo-flow calculation for internal blade cooling rib-roughened passages. The 1-D calculation utilized correlations of friction and heat transfer in the rib-roughened cooling passages derived from large-eddy simulation in ribbed rectangular channels. In this study, effects of inlet temperature profiles, mass flow rate, and temperature of internal cooling air on the blade local temperature are also presented. Coutandin et al. [15] used iterative process involving external fluid dynamic simulations (CFD), internal flow network code and finite element conductive model (FEM) to design an advanced double wall cooling system and validated their results with experimental data. Amaral et al. [16] applied conjugate heat transfer method using 1-D aero-thermal model based on friction and heat transfer correlations for lifetime prediction of a high-pressure turbine blade operating at a very high inlet temperature. Their CHT method is validated on two test cases: a gas turbine rotor blade without cooling and one

with five cooling channels evenly distributed along the camber line.

The abovementioned studies investigated the calculation procedure of blade temperature distribution. Temperature distribution is one of the various loads that affect blade life. For calculating blade life, in addition to temperature, some other conditions and parameters should also be considered. Pressure distribution, rotating velocity and support conditions are some other factors that determine blade life. Furthermore, in order to calculate blade life, failure mechanisms should be identified.

During gas turbine operation, each component has its own failure modes. For instance, vanes failure modes are thermal fatigue, low cycle fatigue and corrosion. In the case of blades, failure mechanisms are low cycle fatigue, high cycle fatigue, thermal fatigue, environmental attack and creep [17,18]. Consequently, life estimation of gas turbine hot section blades consists of two main parts; creep and fatigue calculation and environmental attack consideration. In most life estimation investigations, creep and fatigue lives are major parts of procedure and other failure mechanisms like corrosion are in second order of importance [19,20]. The critical part of a gas turbine that determines the hot section life is the turbine 1st stage blade [17–21]. Severe states of stress and temperature and corrosive condition in gas turbine 1st stage are the reasons for this claim.

There are many studies, which considered the aforementioned failure mechanisms for predicting blade life. Hashemi and Carlton [22] predicted the blade life of a steam turbine by estimating creep and fatigue life as main failure mechanisms. Their life prediction system used a linear damage accumulation method in order to calculate the total life of blade. Greitzer [23] utilized a turbine blade life and durability approach based on variability in design and operating factors. The lifetime was modeled considering thermo-mechanical low cycle fatigue and creep. The study showed that deviation in cooling air temperature was the most important factor determining blade life. Hou et al. [24] used a non-linear FE method to determine the steady state and transient stresses in a blade, and in this manner, determine the cause of failure in fir-tree region. This approach utilized cyclic symmetry model, centrifugal forces due to rotation velocity, and a 3-D temperature distribution. The common cause of failure was shown to be a combination of low cycle fatigue (LCF) and high cycle fatigue (HCF). Castillo et al. [25] also performed a similar blade failure investigation for another gas turbine blade. Their analysis results show that the major part of damages in the hot section blade is due to creep failure.

There are many uncertainties in life simulation of turbine blades. In gas turbine operation, deviation of some parameters from set points can affect hot section life. For example, a blockage or leakage in coolant passage would affect coolant mass flow rate. This can greatly influence hot section temperature distribution and resultant life. Furthermore, some deviations in manufacturing process can affect life. In addition, there are usually some uncertainties in calculations of cycle, turbomachinery and heat transfer parameters, which are crucial boundary conditions for life estimation. Unfortunately, there are a few studies on the effect of aforementioned factors on blade life. Roos [26] conducted a set of sensitivity analysis of the trailing edge ejection slot width on the cooling effectiveness in a cast nozzle guide vane. For internal coolant passage, he utilized a pipe network-based approach. His investigation showed that reducing the slot size causes a corresponding decrease in coolant mass flow rate and consequently an increase in blade temperature. Espinosa et al. [27] evaluated the effect of reducing the cooling airflow rate on the temperature distribution on the blade's surface. The results show a clear dependence of temperature distribution, related to the cooling effectiveness, on the coolant flow rate in the cooling channels. Haubert et al. [28] evaluated effects of design parameters on the predicted blade life. They concluded that the heat transfer parameters are the most critical variables affecting blade life and the least critical parameter was blade geometry.

The main concern of this study is to investigate the effects of some important uncertainties or deviations on blade temperature and life. Cooling inlet boundary conditions that are obtained from secondary air system (SAS) analysis, and material specifications of blade coating, which are specified during the manufacturing process, are some of these deviations. In addition, since mechanical drive gas turbines operate in part load conditions, the effect of change in load on blade temperature and life is also investigated.

2. Procedure description

In this section, procedures used for heat transfer calculation and life estimation are described. In addition, validations of heat transfer and life procedures are explained.

2.1. Conjugate heat transfer procedure

Conjugate heat transfer involves three different physical aspects, flow and heat transfer in external domain and internal cooling passages, and conduction within blade structure. In the conjugate procedure, the calculation of external and internal flow and heat transfer is coupled together with blade conduction. Blade temperature distribution is determined by analyzing these three sections. Results of external flow and heat transfer simulation define external boundary conditions for metal conduction calculation. Internal boundary conditions for the conduction calculation are defined by heat and fluid flow simulation of internal coolant passages. As mentioned in the previous section, 3-D simulation of internally cooled blade heat transfer with complex cooling passages is time-consuming. Therefore, a network method is used for simulation of flow and heat transfer in internal passages.

Figure 1 illustrates conjugate heat transfer algorithm. Calculations of internal and external flow and heat transfer are coupled with blade conduction in an iterative procedure. Using assumed wall temperature, internal flow and heat transfer are calculated. The outcome of this computation is a boundary condition for blade conduction analysis comprising of internal heat transfer coefficient and fluid temperature. The other outcome is coolant properties such as mass flow rate and fluid temperature at cooling outlets. Blade conduction calculation also results in internal flow simulation boundary, namely wall temperature. Reaching convergence, results of blade metal temperature distribution, coolant mass flow rate and temperature are obtained.

It should be mentioned that in this study, three-dimensional external flow and heat transfer simulation along with conduction analysis in solid domain are carried out simultaneously by ANSYS CFX solver. Hence, there is no need to iterate over conduction and external flow analysis. These two domains (solid domain for blade and fluid domain for external flow filed) are meshed and the conjugate procedure was applied by ANSYS CFX solver. Therefore, the simulation has just boundary condition exchange between one-dimensional network code (based on Meitner [29,30]) for internal passages and ANSYS CFX software for conduction and external flow.

2.2. Heat transfer procedure validation

The numerical model for validation purpose is based on experimental study of Hylton et al. [31]. This experiment is the only one known by the authors to exist in the open literature that has conduction within the metal, as well as external flow and internal coolant flow. There are two different geometries in this experiment, namely, C3X and MarkII. In this paper geometry and boundary conditions of C3X has been used. The C3X vane has a constant cross section and its height in span-wise direction is 76.2 mm. It also has ten cooling passages with circular cross section. The geometry specification of C3X vane and its cooling passages can be found in [31]. Simulation has been carried out for run number 112 of the experiment. Imposed boundary conditions for external gas pass and internal cooling channels are the same as experiment and reported in Table 1 and Table 2.

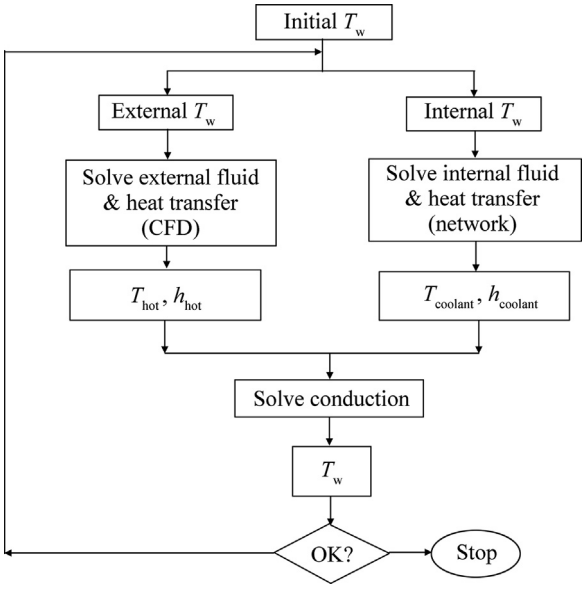

Figure 1 Conjugate heat transfer algorithm.

2.2.1. 1-D simulation of C3X cooling passages

Although cooling passages of C3X vane are simple and it is possible to simulate the whole blade in ANSYS CFX, this vane is used for validation of conjugate process, which is utilized in this study. Each cooling channel of C3X vane is divided into 10 equal elements. The 1-D coolant network has been applied for each cooling channel. The geometry of the blade and its coolant channels' elements are shown in Figure 2.

The flow is assumed to be fully developed in the inlet of holes at hub. The exit pressure of cooling channels is atmospheric pressure. The mass flow rate and inlet temperature for each cooling passage are listed in Table 2.

2.2.2. Grids and solution details for metal and external flow of C3X vane

In order to generate the computational domain, two separate domains for solid and fluid are meshed using ANSYS CFX Mesh. A two-dimensional grid is first created and because the airfoil has constant cross-section, the grid is stacked in the span-wise direction to create the full domain. In order to allow the resolution of thermal boundary layers, stretching is applied in the span-wise direction away from the hub surface of the passage and towards the casing. All wall adjacent grid points are located at y^+ equal to or less

Table 1 External gas pass boundary conditions for C3X simulation.

$P_{t,in}$/kPa	$T_{t,in}$/K	$P_{s,out}$/kPa
321.7	783	192.5

Table 2 Coolant boundary conditions for C3X simulation.

Coolant number	$T_{s,in}$/K	$\dot{m}$/(kg/s)
1	387	0.0078
2	388	0.0066
3	371	0.0063
4	376	0.0067
5	355	0.0065
6	412	0.0067
7	367	0.0063
8	356	0.0023
9	406	0.0014
10	420	0.00068

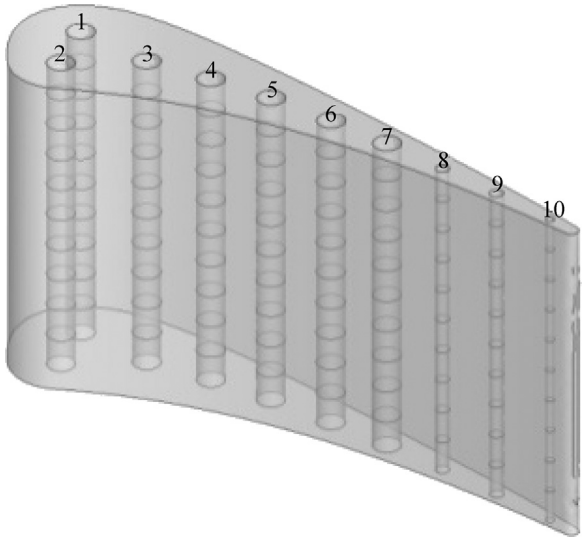

Figure 2 C3X geometry and the 1-D elements of ten coolant channels.

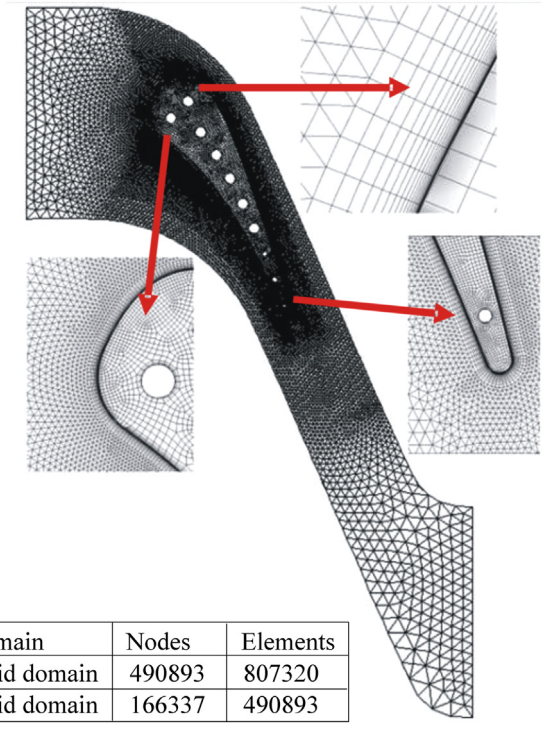

Domain	Nodes	Elements
Fluid domain	490893	807320
Solid domain	166337	490893

Figure 3 View of numerical mesh on plane of constant span-wise coordinates.

than unity to resolve the viscous sub-layer region. A view of the computational mesh on the plane of constant span-wise coordinate and the statistics information about the independent grid are shown in Figure 3.

In the fluid zone, time-average Navier-Stokes equations are solved and shear stress transport (SST) k-ω turbulence model are used. Air is modeled using perfect gas assumption. Mesh interface between solid and fluid consists of non-conforming nodes that require the use of solid-fluid general grid interface (GGI) feature from CFX. In each iteration, at fluid-solid interfaces, energy balance is satisfied. The temperature of the boundary itself is adjusted to meet this condition. Therefore, fluid-solid interfaces are fully coupled and required no user-specified boundary values.

Predicted pressure distribution at the vane mid-span is compared with experimental data in Figure 4. The prediction exhibits excellent agreement with the experimental results, validating the aerodynamic portion of the model.

Predicted distribution of non-dimensional temperature on the external surface of the vane on the mid-span plane is compared with the experimental data in Figure 5. On the pressure side ($-1 < X/C_a < 0$) results show reasonable

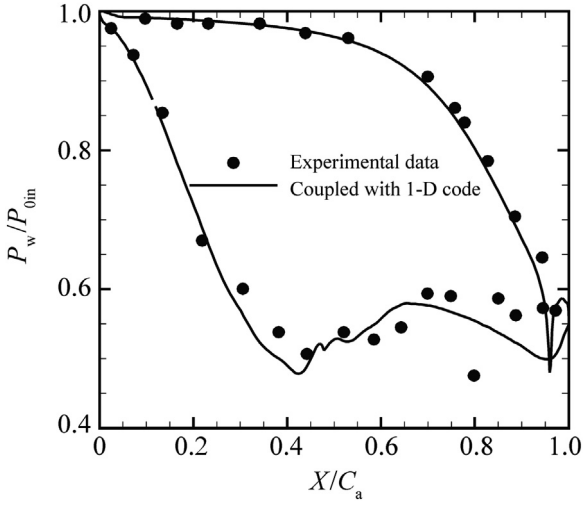

Figure 4 Predicted and measured pressure distribution on the mid-span plane.

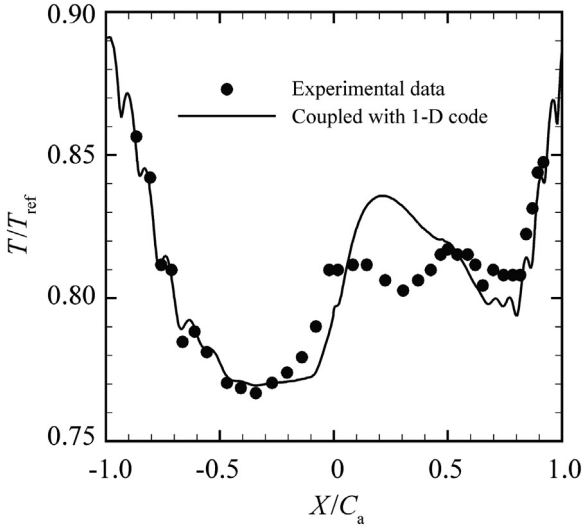

Figure 5 The non-dimensional temperature distribution on mid-span plane.

agreement with the experimental data and there is an under-estimation of wall temperature for $-0.2 < X/C_a < 0$. On the suction side, there is an over-estimation for $0.1 < X/C_a < 0.5$. It should be noted that the average error for the whole data is around 1%. The error of maximum temperature that is located in the trailing edge region is 0.6% and the error of average blade temperature is 0.14%. Therefore, the results show that the errors are within a reasonable range.

2.3. Life estimation procedure

Gas turbines hot section blades are subjected to simultaneous action of gas pressure coming from the combustion chamber, centrifugal forces in the case of the rotor blades and severe temperature transients. These combined parameters cause a high state of stress involving several complex mechanisms of damage, such as creep, fatigue caused by mechanical and thermal stress fluctuations. In this work, fatigue and creep lives are calculated by the Manson-Coffin equation and Larson-Miller model, respectively. The Miner linear model also evaluates complex damage accumulation.

2.3.1. Life prediction for fatigue

Manson-Coffin [32–34] recognized that the cyclic strain is related to the number of cycles to failure, by the equation:

$$\frac{\Delta\varepsilon}{2} = \frac{\sigma_f}{E}(2N_f)^b + \varepsilon_f(2N_f)^c \quad (1)$$

where N_f is the number of cycles to failure, E is the elasticity modulus, σ_f fatigue strength coefficient, ε_f fatigue ductility coefficient, and b and c fatigue strength exponent and fatigue ductility exponent, respectively [32,33].

2.3.2. Life prediction for creep

Creep damage is the most important failure mechanism for turbine blades. When turbine materials are exposed to stress and operating above a certain temperature, they undergo plastic deformation known as creep. In the present work, creep for metal is described by the Larson-Miller parameter (LMP):

$$LMP = T\frac{\log(t_r) + C}{1000} \quad (2)$$

where T is temperature in Kelvin, t_r is the time to creep rupture in hours. The C coefficient is taken equal to 20 [34].

2.3.3. Model for fatigue-creep interaction

In this work, in order to take into account the interaction between fatigue and creep at varying temperatures, the Miner's damage accumulation model is used:

$$\sum\frac{n_i}{N_i} + \sum\frac{t_j}{t_{rj}} = D \quad (3)$$

According to this equation, when damage accumulation (D) reaches the unity, the damage results to failure [35]. Figure 6 shows the flow chart of the life estimation procedure which is used in this investigation.

2.4. Life procedure validation

In order to validate the creep model, the stress-rupture test condition of IN792 is imported into the Larson-Miller creep model and finally the results compared with test data. Figure 7 shows the comparison between calculated and test data. As shown, in stress values below 200 MPa, the calculated results have good agreement with the test data. The critical region in the test case used in the present work has stress values below 200 MPa and this region determines the blade life. Since the maximum deference between test data and calculated creep life (Figure 7) at 200 MPa is less than 500 hours, using this approach for life calculation would be acceptable.

The best approach for validating life results is to test the blade in actual operating condition. Testing in real condition entails great cost and time; therefore, in the present investigation, the life method is validated by comparing the results with reference [36]. In this respect, the effect of load variation on life factor is selected to compare. Figure 8 shows the relation between power level and life factor for clean engine, reported by Gas Path Analysis Limited (GPAL) Institute [36] compared with calculated results. As shown, the calculated data has good agreement with the reported data. The maximum error occurs at power level of 90%, which the difference is 7.4%.

3. Results and discussion

The present work aims to investigate effects of different parameters on the blade life in a typical high pressure, high temperature turbine blade with internal convection cooling. The case study for heat transfer simulations is the first stage rotor blade of a mechanical drive gas turbine, which has complicated internal cooling passages. In this blade, coolant flow ejects from trailing edge and tip. Several details are

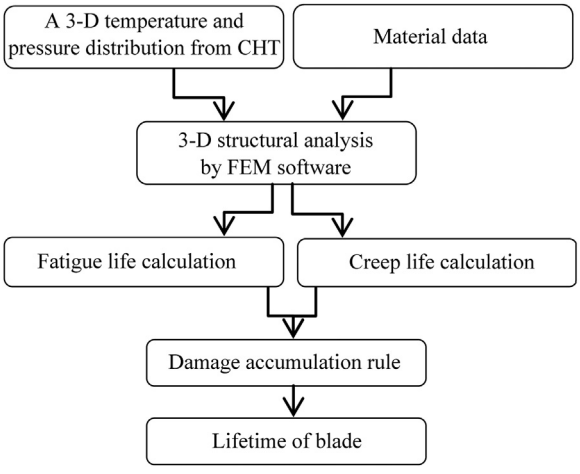

Figure 6 Flow chart of the life estimation procedure.

depicted in the computer aided design (CAD) model of the blade shown in Figure 9. As can be noted, the blade is shrouded.

In heat transfer calculations, in order to investigate effects of stator on the rotor flow and heat transfer, the whole stage is simulated. Since the main target is only to investigate the rotor heat transfer, the stator is simulated with adiabatic boundary condition and its coolant injects to mainstream from its trailing edge. In this modeling for stator, whole energy balance is conserved without detailed cooling structure. It should be noted that the upstream fluid flow in the stator and the stator-rotor interaction affect the final blade temperature; consequently, it is required to set up hot gas domain including whole stage. By this method, the flow direction and radial profile of pressure and temperature at the inlet plane of the rotor is perfectly assigned. The ratio of stator number to the rotor one is about 1:1. The stage model is used for treating stator/rotor interaction. Periodicity conditions to replicate the multiple passages are employed and therefore only one blade is included in computations. For fluid domains, all wall adjacent grid points are located at y^+ equal to or less than unity to resolve the viscos sub-layer region. All calculations are based on three-dimensional, compressible fluid flow. The transport properties such as viscosity and thermal conductivity are functions of temperature. For the spatial discretization, a second-order scheme is used. In the simulation, SST k-ω turbulence model is used in the fluid zone.

The stage operating conditions and coolant inlet and outlet boundary conditions for the reference case are given in Table 3. These data are obtained from cycle simulation of whole gas turbine and SAS analysis. In addition, the geometry specifications and blade metal density, thermal conductivity and specific heat are listed in Table 4.

Flow and heat transfer within the stage predicted with conditions given in Table 3. For the reference case, contours of blade temperature and flow field and metal temperature distribution at 70% span are shown in Figure 10 and Figure 11, respectively. It can be seen that in the blade root, metal temperature is about coolant temperature and maximum temperature occurs at the leading edge. Since inclined ribs and pin-fins have been used in the blade trailing edge, it is not a critical region from heat transfer point of view. Because the maximum value of inlet temperature radial profile occurs at 70% span of leading edge, maximum blade temperature occurs at this span-wise location.

3-D stress analysis on the blade is carried out using ANSYS commercial software. This analysis is based on a set of input data, which includes material properties (Table 5), 3-D temperature and pressure distributions on the blade, and the operational conditions listed in Table 3.

The 3-D model consists of approximately 267000 solid elements comprised of more than 437000 nodes. It includes all relevant details of the internal cooling channels, the shank and the root attachment. Thermal-mechanical stress

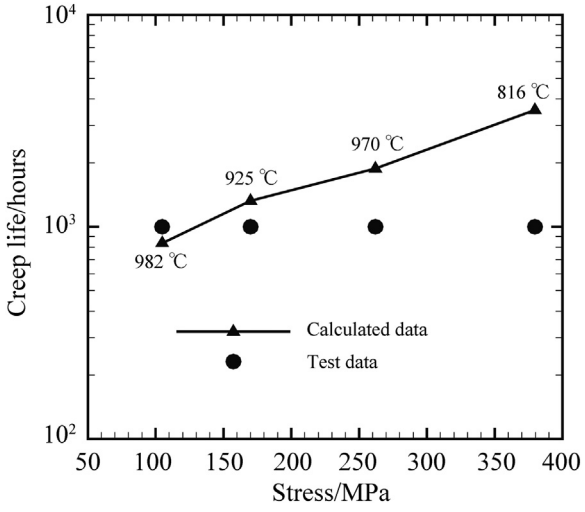

Figure 7 Comparison between calculated and test data for creep life model validation.

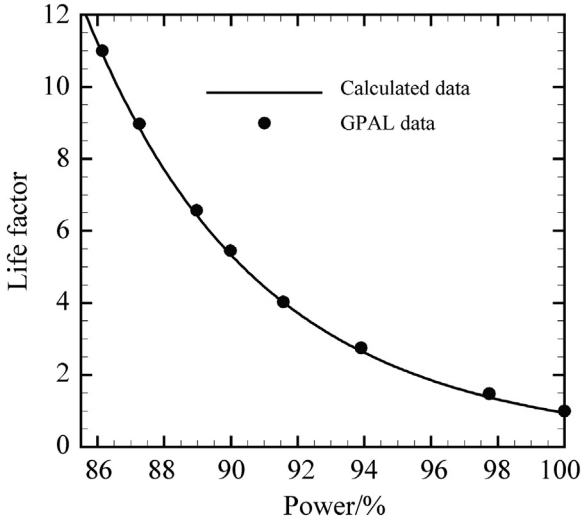

Figure 8 Comparison between GPAL reported and calculated data.

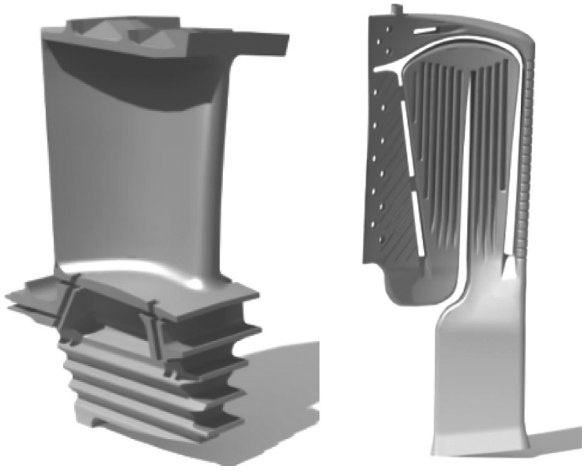

Figure 9 CAD model of simulated blade and its internal cooling passages.

calculations are conducted by applying calculated temperatures throughout the bucket. The centrifugal load for the reference case is also applied to account for the mechanical load. The temperature dependent anisotropic material properties are used for the IN792 material (Table 5).

The calculated stress distribution for the reference case is shown in Figure 12. The highest equivalent stress—Von Mises—occurs near the platform at fir-tree region. This area would be the most susceptible to thermal-mechanical fatigue.

A stress-rupture criterion and associated Larson-Miller parameter are commonly used to evaluate creep life. Contour plot of creep life distribution for the reference case is shown in Figure 13. As seen, the lowest value of creep life is occurred in the mid-span of airfoil at the leading edge. With regard to this, the critical point of creep life usually occurs near the temperature maximum value (see Figure 11). It means that the creep life is strongly influenced by the blade temperature distribution.

The fatigue life analysis is carried out based on Manson-Coffin method and the results of stress analysis (Figure 14). The considered fatigue cycle in this study is startup and shut down cycle. As shown in Figure 14, from the fatigue life point of view, the blade most critical area is root and fir-tree zone. According to Figure 14, it can be realized that the minimum value of fatigue life occurs at the same point as the maximum value of stress. It means that, the blade stress is the determinant parameter in fatigue life. However, in the case of creep life, blade temperature has the greater impact than stress.

Table 3 Stage operating conditions (reference case).

Parameter	Value
$T_{t,in}$/K	1484
$P_{t,in}$/kPa	1382 (13.82 bar)
$P_{s,out}$/kPa	647 (6.47 bar)
$P_{t,in\text{-}c}$/kPa	1420 (14.2 bar)
$T_{t,in\text{-}c}$/K	696
Speed/rpm	9800

Table 4 Rotor blade metal and coating specifications (reference case).

Parameter	Value
ρ_{me}/(kg/m^3)	8250
k_{me}/(W/(m · K))	17.7
C_{me}/(J/(kg · K))	710
ρ_{co}/(kg/m^3)	6000
k_{co}/(W/(m · K))	2.29
C_{co}/(J/(kg · K))	470
δ_{co}/μm	10

4. Sensitivity analysis

In this section, a study of which variables most affect the blade life for a typical high pressure, high temperature turbine blade with internal convection cooling is conducted. It should be mentioned that the sensitivity analyses are carried out using the aforementioned approaches. Four variables chosen for temperature and life sensitivity analysis are: blade coating thickness, coolant inlet pressure and temperature (as a result of secondary air system), and load variation. The typical range of variations for these variables is determined from engine running conditions and the standard deviations in the manufacturing process. These four variables and their variations are listed in Table 6.

Effects of these variables on the blade temperature are determined using conjugate heat transfer procedure on four parameters of the blade temperature distribution, namely: (1) average blade temperature, (2) maximum blade temperature, (3) average pressure and suction sides temperature, and (4) average shroud temperature. In addition, the effects of these variables on the blade life are illustrated.

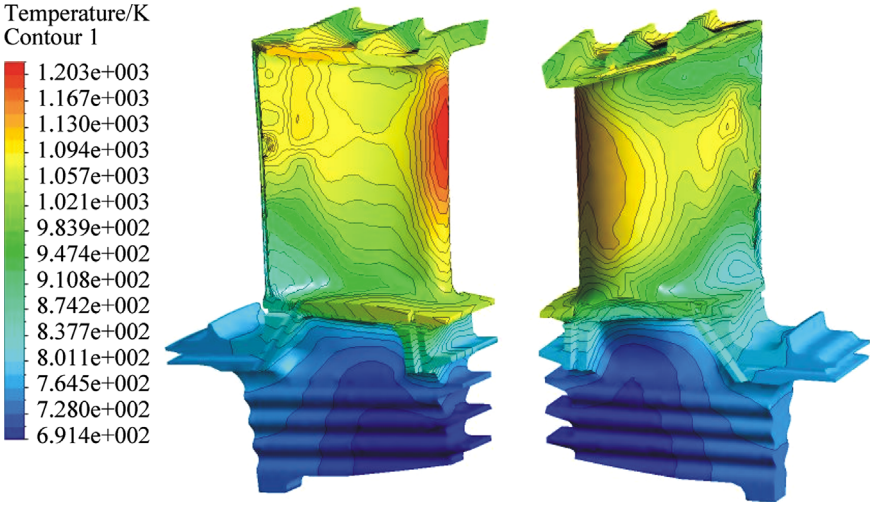

Figure 10 The blade temperature distribution for reference case.

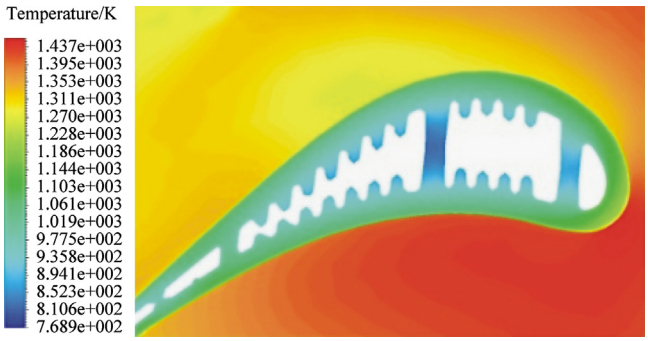

Figure 11 Flow field and metal temperature distribution at 70% span.

Table 5 Mechanical properties of IN792 superalloy [37].

Parameter	$T_1=21$ °C	$T_2=540$ °C	$T_3=980$ °C
$\rho_{me}/(kg/m^3)$	8250	–	–
E/GPa	201	172	145
α/K^{-1}	11.6	14	–
υ	0.3	0.3	0.3

The results are compared to the reference case and shown in the following subsections.

4.1. TBC thickness

Thermal barrier coating (TBC) is an essential requirement of a modern gas turbine engine to provide thermal insulation to the turbine blades. The consequent reduction of temperature helps in prolonging the life of the metal alloy. Coating thickness is one of the main characteristics of TBC, which considerably affect blade temperature and life. In this section, effects of this parameter on the blade temperature distribution and resultant life are investigated. Rotor blade temperature variation versus coating thickness is plotted in Figure 15.

Temperature variation with coating thickness is to some extent linear. As can be seen, the coating thickness has significant effect on the blade temperature especially on the blade external surfaces on the pressure and suction sides.

Effect of adding ceramic coating and its thickness on blade creep life is also studied. As can predict form temperature results (Figure 15), adding the thermal barrier coating on blade surface can greatly increase the creep life. Figure 16 defines the creep life of blade corresponding to the changes in TBC thickness. As can be seen, adding 300 μm TBC on the blade leads to 9 times increase in life in comparison with the reference case (100 μm TBC). In other words, the thickness of TBC has great effect on blade life and so, loss of coating may result in catastrophic failures and horrible damages in turbine.

4.2. SAS pressure and temperature

SAS provides the cooling air needed to keep metal temperature of components in the hot gas section below

Figure 12 Stress analysis results for 1st stage blade.

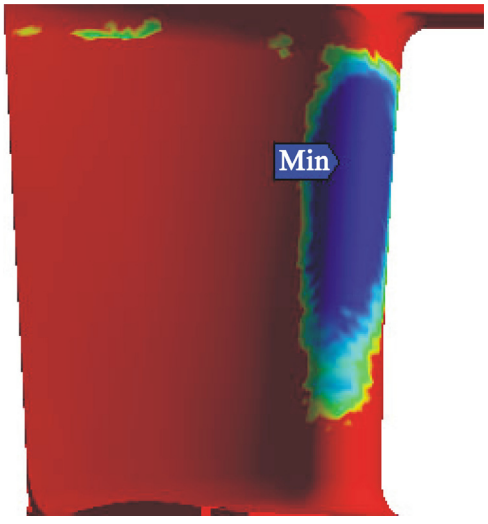

Figure 13 Creep life distribution on the blade for the reference case.

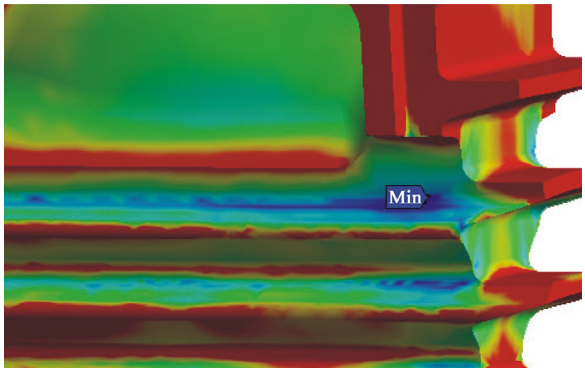

Figure 14 Fatigue life analysis result and critical zone.

Table 6 Assumed variables for sensitivity analysis.

Variable	Range of variation
δ_{co}/μm	10–300
$P_{in\text{-}c}$ rotor	5%–10% decrease
$T_{in\text{-}c}$ rotor	0–5% increase
Load/%	60%–100%

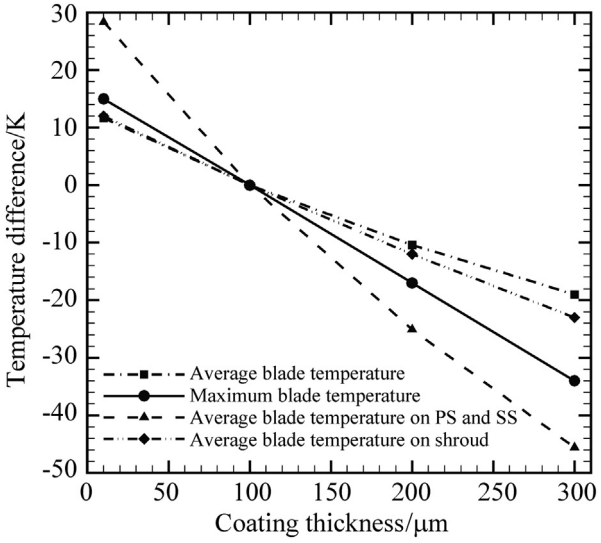

Figure 15 The rotor blade temperature variation versus coating thickness.

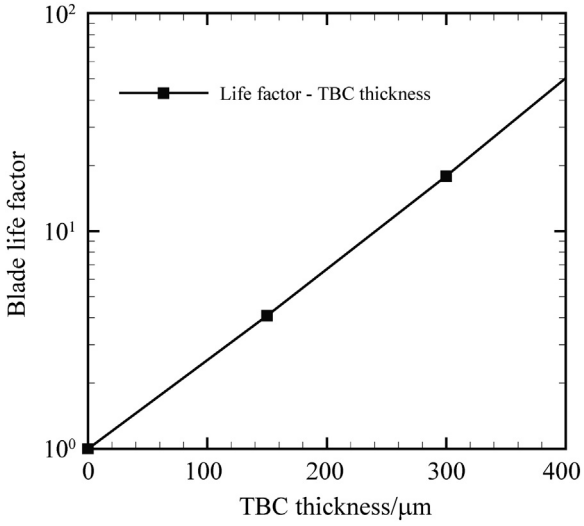

Figure 16 Effect of TBC coating on blade creep life.

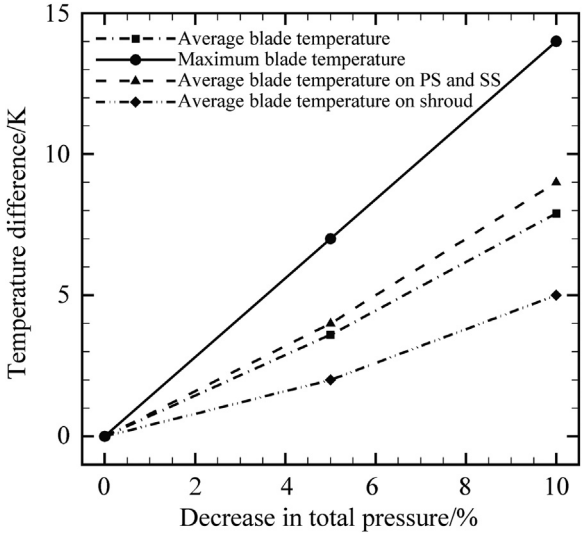

Figure 17 The blade temperature variation versus pressure drop at the coolant inlet.

the maximum allowable. As fluid flow passes through SAS, its pressure reduces and its temperature increases. In this section, the effects of SAS pressure loss and temperature rise on blade temperature and life are investigated. Figure 17 shows the effect of SAS pressure drop on the blade temperature. It is obvious that the reduction of the blade cooling inlet pressure causes coolant mass flow to decrease. As a result, the amount of heat transferred to coolant decreases and blade average temperature increases. Based on the illustrated results, it can be realized that 10% SAS pressure loss can result in 14 K increase in maximum blade temperature.

Blade temperature variation is plotted against coolant inlet temperature in Figure 18. As shown in this figure, the blade temperature varies linearly with inlet total temperature. Moreover, 5% increase in inlet coolant temperature results in 10 K rise in maximum blade temperature.

Secondary air pressure reduction causes the blade temperature to increase and then blade life severely decreases. Figure 19 shows the relation between SAS pressure drop and blade life factor.

In the similar manner, blade lifetime is seriously depended upon the imposed temperature and stress level and any changes in these parameters can results in life limit. According to Figure 20, 5% augmentation of SAS

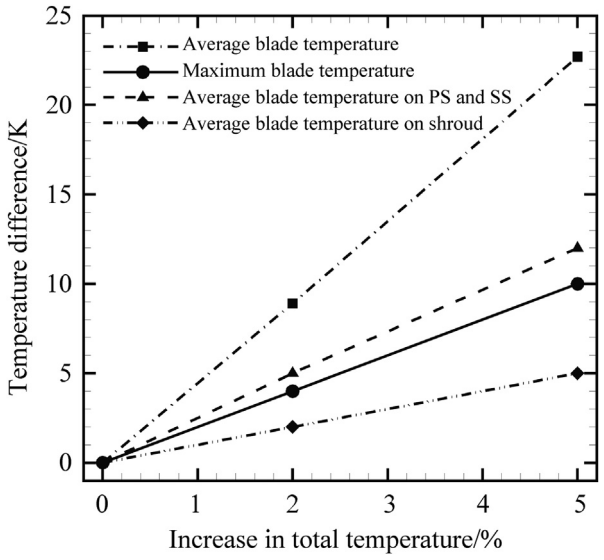

Figure 18 Blade temperature variations versus coolant inlet temperature.

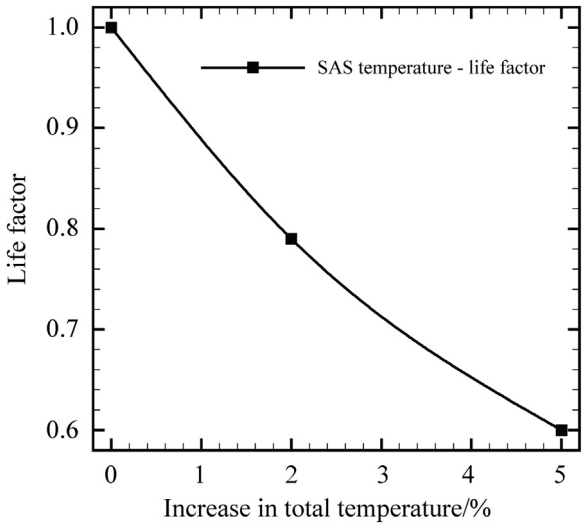

Figure 20 Effect of secondary air system temperature on blade life factor.

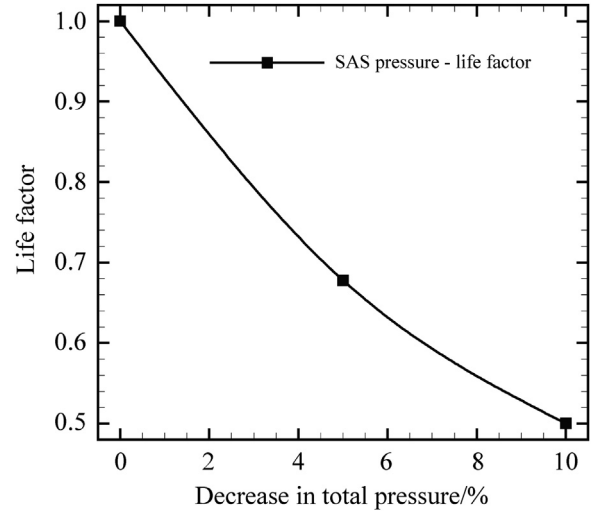

Figure 19 Effect of secondary air system pressure on blade life factor.

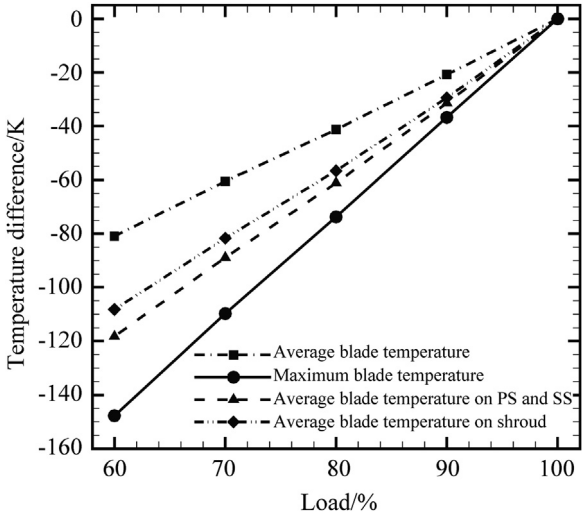

Figure 21 Effect of load variation on blade temperature.

temperature causes the blade life factor to drop to 0.6. Since 5% increase in cooling air temperature means 10 K increment in blade maximum temperature (Figure 18), this causes blade creep life to decrease 40%.

Comparison between Figure 17 and Figure 18 reveals that 5% decrease in SAS pressure has less effect on blade maximum temperature than 5% increase in SAS temperature. Accordingly, it can be concluded that the influence of SAS temperature rise on blade life is of great importance. Figure 19 and Figure 20 confirm this claim.

4.3. Load variation

Operating at part load or peak load are common situations in mechanical-drive applications of gas turbines. In fact, one of the most important factors that determines the blade steady state lifetime is gas turbine load. In view of the harmful effects of peak loading, part load operation is a simple way to counterbalance the negative influences of peak load. For the case studied in the present work, effect of load change on blade temperature is shown in Figure 21. This figure shows that 40% decrease in load results in falling blade temperature by 150 K. Contours of blade temperature at different loads are depicted in Figure 22. It can be noted that temperature distributions have not greatly changed as a result of load variation and just the temperature values differs at different loads.

The effect of part load operation on the lifetime of turbine blade is shown at Figure 23. One of the interesting points that can be realized is that 300 hours operation at 70% load is equal to one hour operation at base load. This is mainly

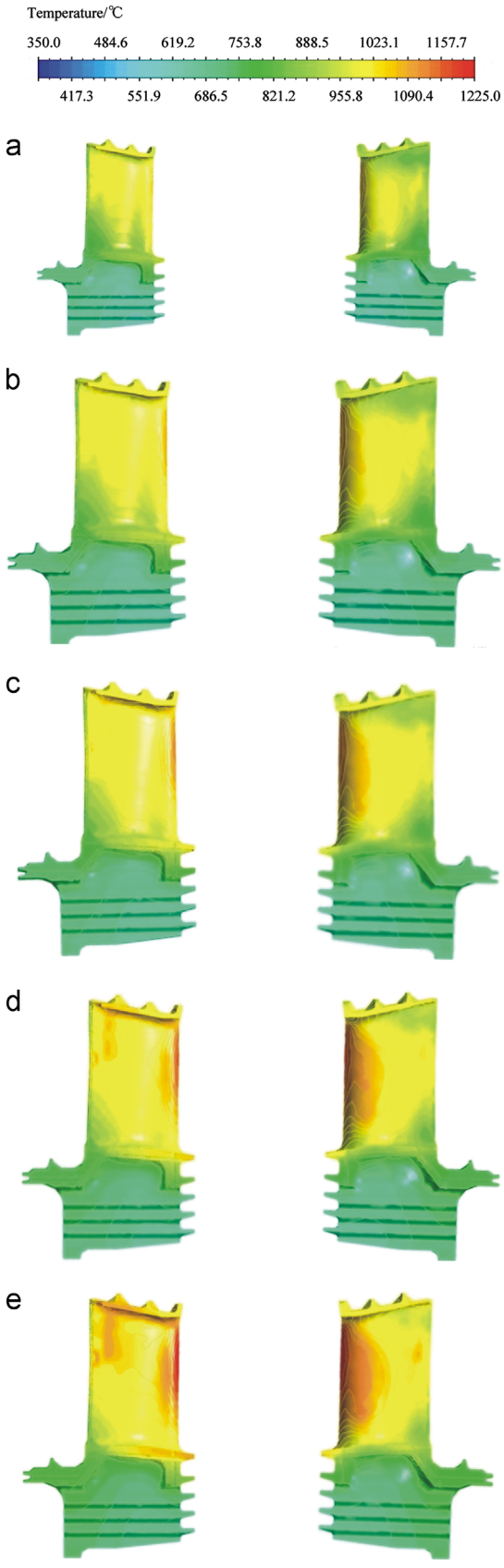

Figure 22 Effect of load variation on blade temperature distribution. (a) 60% load, (b) 70% load, (c) 80% load, (d) 90% load and (e) 100% load.

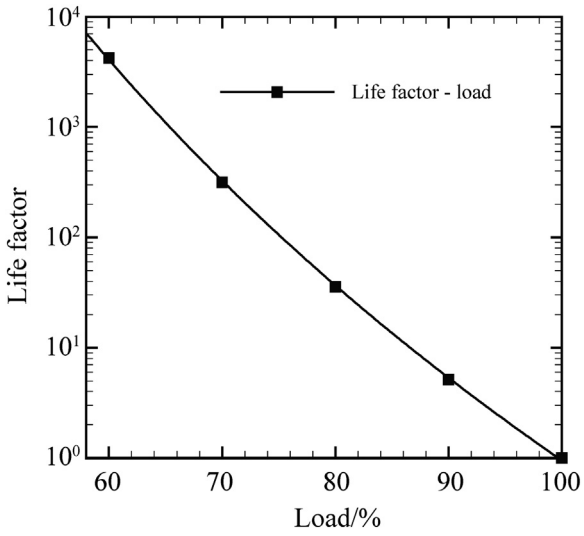

Figure 23 Blade life factor in various operating loads.

because of temperature fall at 70% load in comparison with base load. Engine manufacturers normally quote engine life when the engine is operating at 100% power at International Organization for Standardization (ISO) conditions. However, gas turbines rarely operate at ISO ratings. If an engine operates at 90% load at ISO conditions then the turbine creep life will be 5 times as much as 100% load at the same conditions (see Figure 23). It means that reducing the loading level in mechanical drive applications can increase the reliability and availability of gas turbines.

5. Conclusion

In this study, numerical methodologies for conjugate heat transfer and life estimation are developed and validated against experimental data. The results of both heat transfer and life show good agreement with experimental data. The methods are developed to improve the fidelity of durability analyses for internally cooled airfoils.

Heat transfer and life through typical turbine blade are predicted and the computational results are fully analyzed. The heat transfer results show that maximum blade temperature at the reference case is 960 ˚C and because of inlet temperature radial pattern, occurs at 70% span of blade leading edge. In addition, the life estimation results demonstrate that the minimum life occurs at the same point as maximum temperature. This indicates that the most dominant factor for blade creep life is temperature. Furthermore, the weakest point for fatigue failure mechanism is the fir-tree region of the blade.

Uncertainties of some parameters, which affect turbine blade temperature and life, are also investigated. Results show that adding 300 μm TBC coating on the blade leads to 9 times increase in life in comparison with the reference case (100 μm TBC). In addition, deviation in SAS temperature

has profound effect on the blade life. Furthermore, change of loading level in mechanical drive application gas turbines can increase the reliability and availability.

References

[1] D.E. Bohn, C. Tummers, Numerical 3-D conjugate flow and heat transfer investigation of a transonic convection-cooled thermal barrier coated turbine guide vane with reduced cooling fluid mass flow, ASME Paper No. GT2003-38431, 2003.

[2] W.D. York, J.H. Leyek, Three-dimensional conjugate heat transfer simulation of an internally-cooled gas turbine vane, ASME Paper No. GT2003-38551, 2003.

[3] J. Luo, E.H. Razinsky, Conjugate heat transfer analysis of a cooled turbine vane using the V2F turbulence model, ASME Journal of Turbomachinery 129 (4) (2007) 773–781.

[4] G.A. Ledezma, G.M. Laskowsky, A.K. Tolpadi, Turbulence model assessment for conjugate heat transfer in a high pressure turbine vane model, ASME Paper No. GT2008-50498, 2008.

[5] Z.F. Wang, P.G. Yan, Z.Y. Guo, W.J. Han, BEM/FDM conjugate heat transfer analysis of a two-dimensional air-cooled turbine blade boundary layer, Journal of Thermal Science 17 (3) (2008) 199–206.

[6] Q. Wang, Z.Y. Guo, C. Zhou, G.T. Feng, Z.Q. Wang, Coupled heat transfer simulation of a high-pressure turbine nozzle guide vane, Chinese Journal of Aeronautics 22 (3) (2009) 230–236.

[7] Z. Wang, P. Yan, H. Huang, W. Han, Coupled BEM and FDM conjugate analysis of a three-dimensional air-cooled turbine vane, ASME Paper No. GT2009-59030, 2009.

[8] K. Kusterer, D. Bohn, T. Sugimoto, R. Tanaka, Conjugate calculations for a film-cooled blade under different operating conditions, ASME Paper No. GT2004-53719, 2004.

[9] A. Sipatov, L. Gomzikov, V. Latyshev, N. Gladysheva, Three dimensional heat transfer analysis of high pressure turbine, ASME Paper No. GT2009-59163, 2009.

[10] L. Mangani, M. Cerutti, M. Maritano, M. Spel, Conjugate heat transfer analysis of NASA C3X film cooled vane with an object-oriented CFD code, ASME Paper No. GT2010-23458, 2010.

[11] R.H. Ni, W. Humber, G. Fan, P.D. Johnson, J. Downs, J.P. Clark, P.J. Koch, Conjugate heat transfer analysis of a film-cooled turbine vane, ASME Paper No. GT2011-45920, 2011.

[12] R. Dewey, H. Hulshof, Combustion turbine F-class life management: general electric FA first stage blade analysis, EPRI Solutions, Palo Alto, CA, 2000, 1000318.

[13] S. Zecchi, L. Arcangeli, B. Facchini, D. Coutandin, Features of a cooling system simulation tool used in industrial preliminary design stage, ASME Paper No. GT2004-53547, 2004.

[14] T. Takahashi, K. Watanabe, T. Sakai, Conjugate heat transfer analysis of a rotor blade with rib-roughened internal cooling passages, ASME Paper No. GT2005-68227, 2005.

[15] D. Coutandin, S. Taddei, B. Facchini, Advanced double wall cooling system development for turbine vanes, ASME Paper No. GT2006-90784, 2006.

[16] S. Amaral, T. Verstraete, R. Van den Braembussche, T. Arts, Design and optimization of the internal cooling channels of a HP turbine blade, part I: methodology, ASME Journal of Turbomachinery 132 (2010) 021013–021017.

[17] S.T. Arvanitis, Y.B. Symko, R.N. Tadros, Multiaxial life prediction system for turbine components, ASME Journal of Engineering for Gas Turbines and Power 109 (1) (1987) 107–114.

[18] B. Weber, H. Jin, R. Pistor, P. Lowden, Application of an integrated engineering approach for LM1600 blade life on-line assessment, 16th Symposium on Industrial Application of Gas Turbines (IAGT), Canada, 2005.

[19] M.H. Sabour, R.B. Bhat, Lifetime prediction in creep-fatigue environment, Journal of Materials Science 26 (3) (2008) 563–584.

[20] R. Ohtani, T. Kitamura, M. Tsutsumi, H. Miki, Initiation and growth of small cracks in creep fatigue of an oxide dispersion-strengthened superalloy at elevated temperature, Asian Pacific Conference of Fracture and Strength, Japan, 1993.

[21] N.D. DiMatteo, ASM Handbook: Fatigue and Fracture, ASM International (OH), 1996.

[22] Y. Hashemi, R.G. Carlton, Experience of life assessment of high temperature steam turbine components, International Power Generation Conference, Atlanta, 1992.

[23] A. Kountras, Probabilistic analysis of turbine blade durability, Thesis (S.M.), Massachusetts Institute of Technology, Department of Aeronautics and Astronautics, Massachusetts, 2004.

[24] J. Hou, B.J. Wicks, R.A. Antoniou, An investigation of fatigue failures of turbine blades in a gas turbine engine by mechanical analysis, Journal of Engineering Failure Analysis 9 (2) (2002) 201–211.

[25] R. Castillo, A.K. Koul, E.H. Toscano, Lifetime prediction under constant load creep conditions for a cast Ni-base superalloy, ASME Journal of Engineering for Gas Turbine and Power 109 (1) (1987) 99–106.

[26] T. Roos, NGV trailing edge ejection slot size sensitivity study, ISABE-2005-1158, 2005.

[27] F.Z.S. Espinosa, J.C. Han, A.U. Portugal, J. Kubiak, D. Narzary, S. Blake, F. Cadena, H. Lara, J. Nebradt, Influence of cooling flow rate variation on gas turbine blade temperature distributions, ASME Paper No. GT2008-50103, 2008.

[28] R.C. Haubert, H.M. Maclin, M.E. Noe, E.S. Hsia, R.O. Brooks, High pressure turbine blade life sensitivity, AIAA-80-1112, 1980.

[29] P.L. Meitner, Computer code for predicting coolant flow and heat transfer in turbomachinery, NASA TP-2985, AVSCOM TP 89-C-008, 1990.

[30] P.L. Meitner, Procedure for determining 1-D flow distributions in arbitrarily connected passages without the influence of pumping, ASME Paper No. GT2003-38061, 2003.

[31] L.D. Hylton, M.S. Mihelc, E.R. Turner, D.A. Nealy, R.E. York, Analytical and experimental evaluation of the heat transfer distribution over the surfaces of turbine vanes, NASA Report No. CR-168015, 1983.

[32] R.I. Stephens, A. Fatemi, R.R. Stephens, H.O. Fuchs, Metal Fatigue in Engineering, John Wiley and Sons, Inc., New York, 2001.

[33] J. Schijve, Fatigue of Structures and Materials, Kluwer Academic Publishers, Netherlands, 2003.

[34] V.S. Zeravcic, G. Bakic, D. Markovic, D. Milenkovic, M. Dukic, RCM in power plant practice illustrated on

observation of material aging and defining of component life exhaustion, International Conference of Power-Gen Middle East, AbuDhabi UAE, 2004.
[35] J.A. Collins, Failure of Materials in Mechanical Design: Analysis, Prediction, Prevention, John Wiley and Sons, Inc., New York, 1993.
[36] ⟨http://www.GPAL.co.uk⟩ (GPAL Gas Turbine Simulator - Gas Path Analysis Limited).
[37] M.J. Donachie, S.J. Donachie, Superalloys: A Technical Guide, ASM International (OH), 2002.